

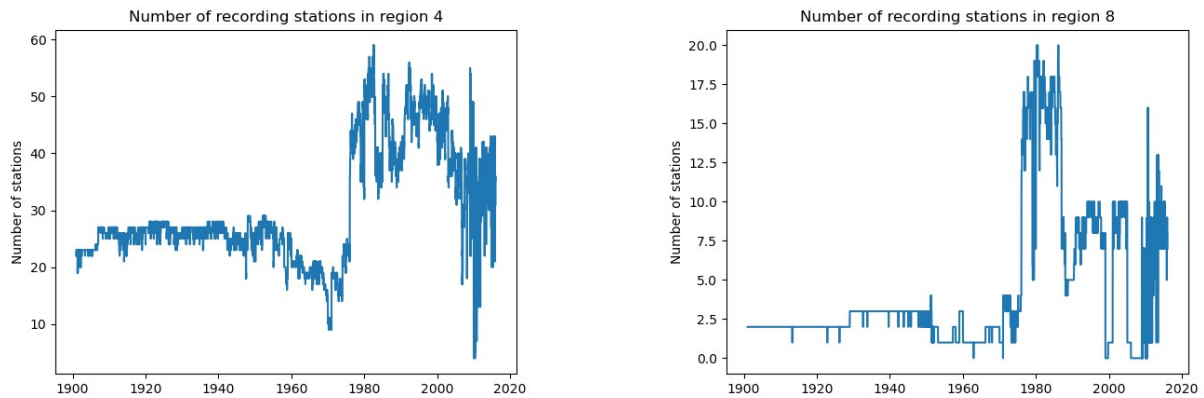
# The rise of Indian summer monsoon precipitation extremes and its correlation with long-term changes of climate and anthropogenic factors

Renaud Falga and Chien Wang\*

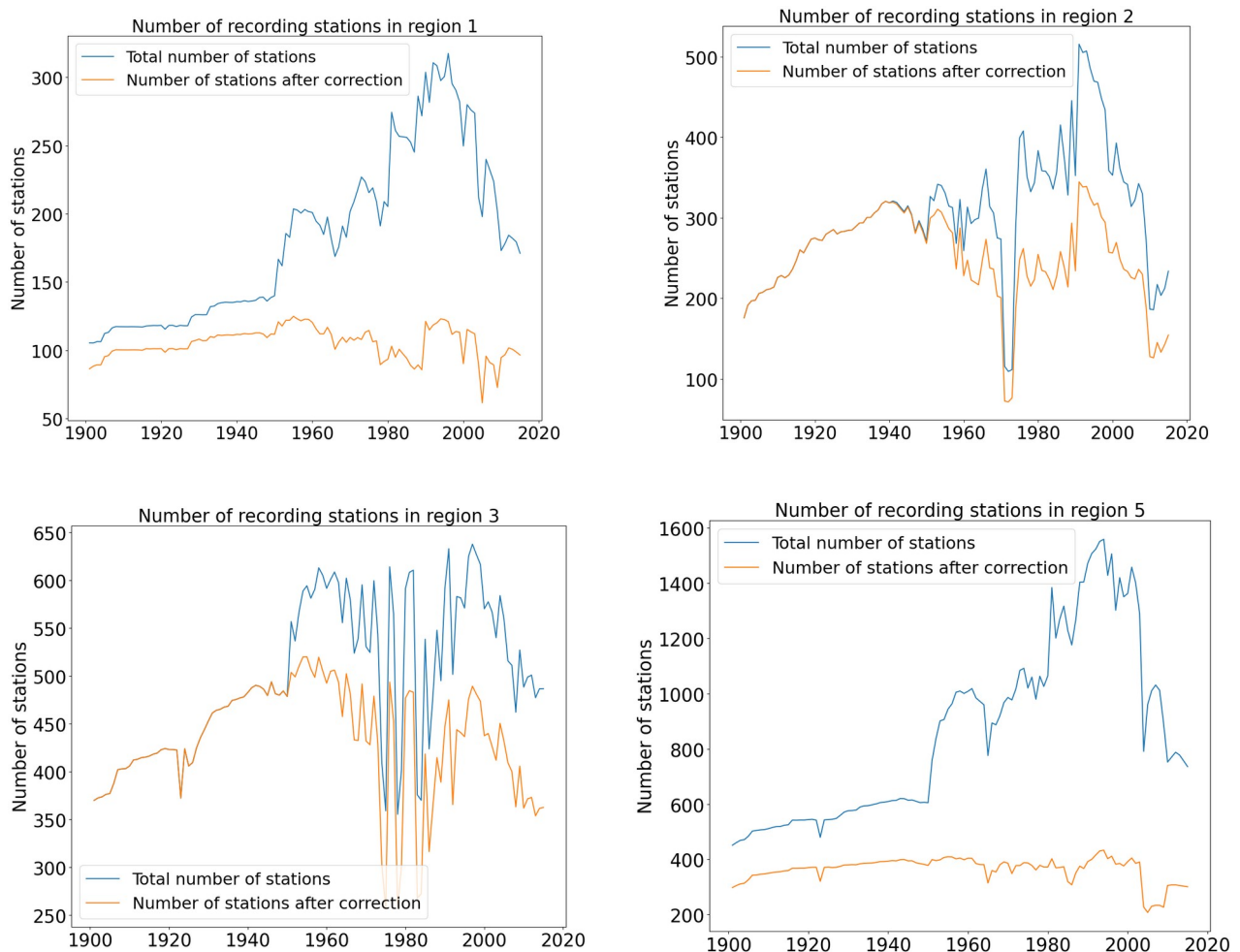
Laboratoire d'Aérodologie, University of Toulouse III – Paul Sabatier, Toulouse, France

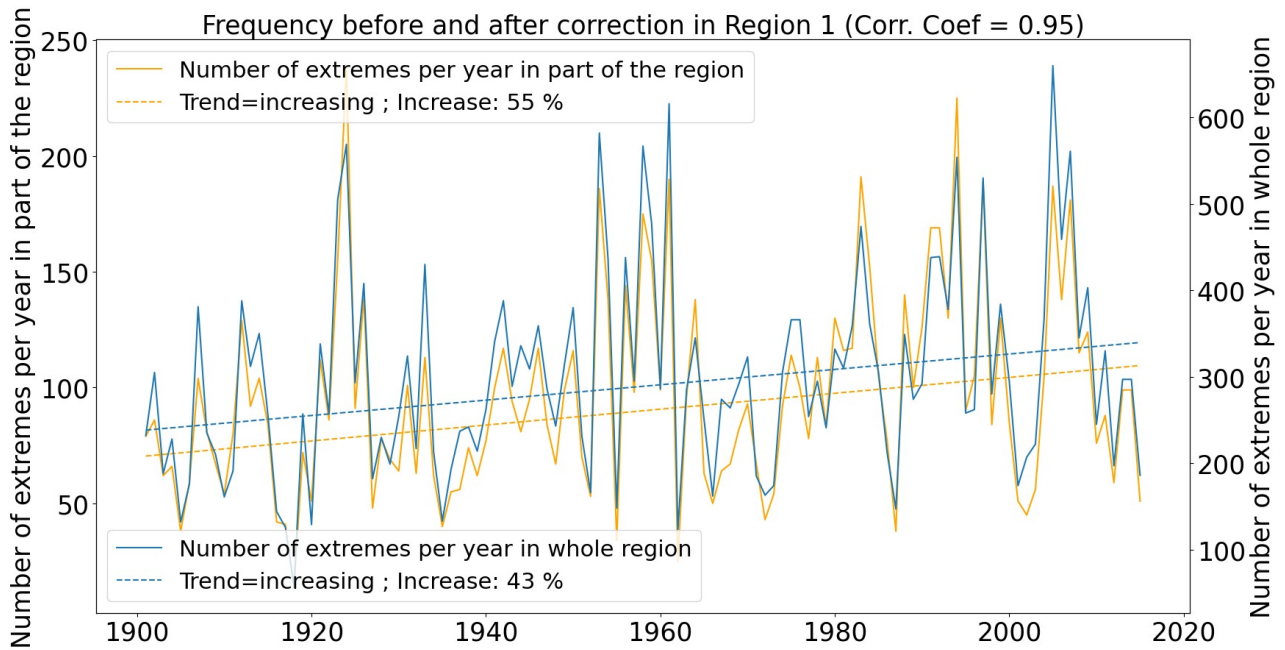
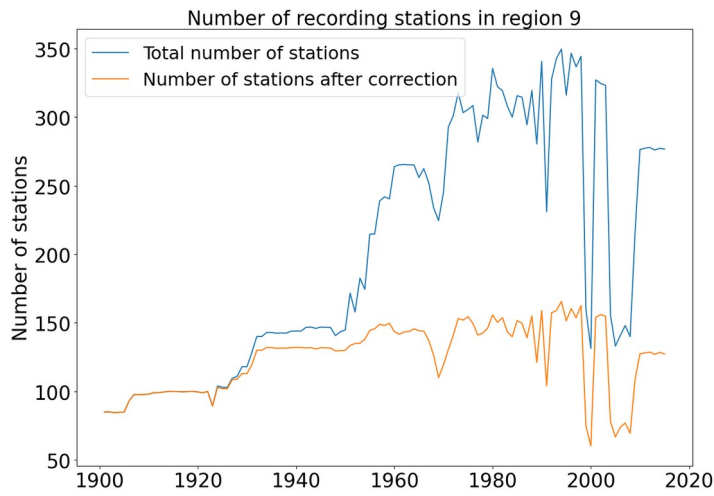
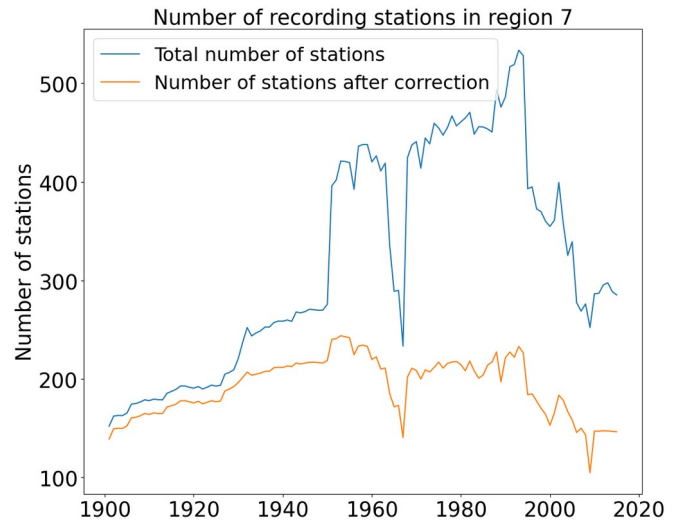
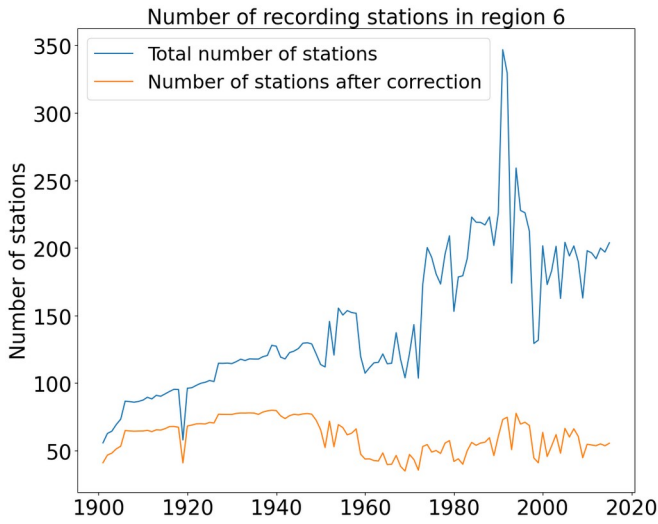
\* email: [chien.wang@aero.obs-mip.fr](mailto:chien.wang@aero.obs-mip.fr)

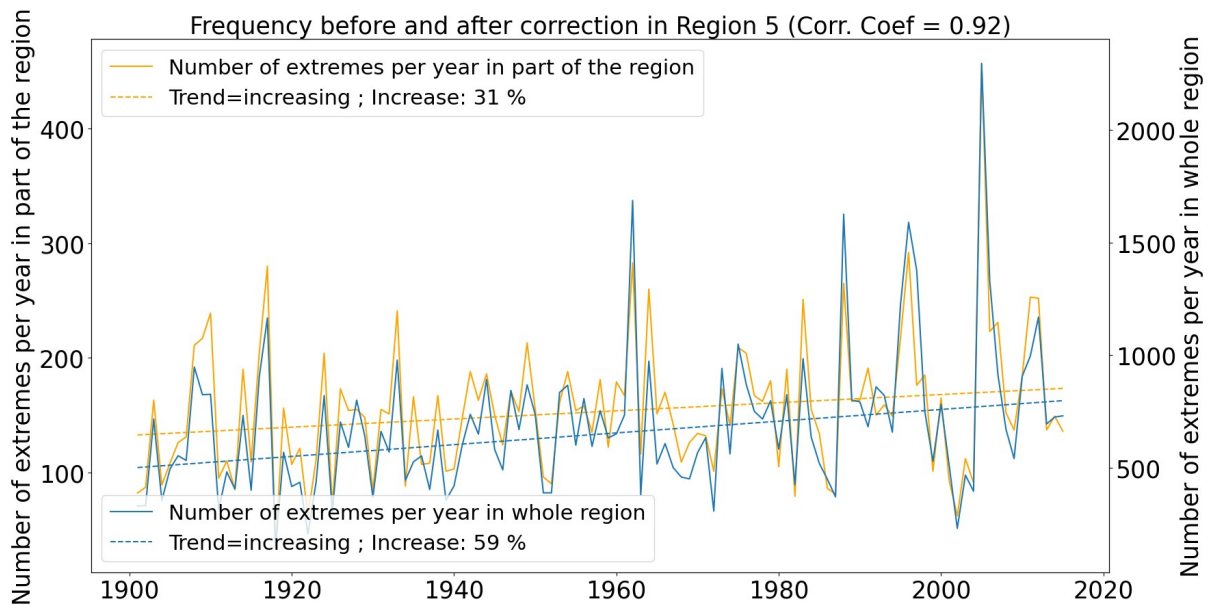
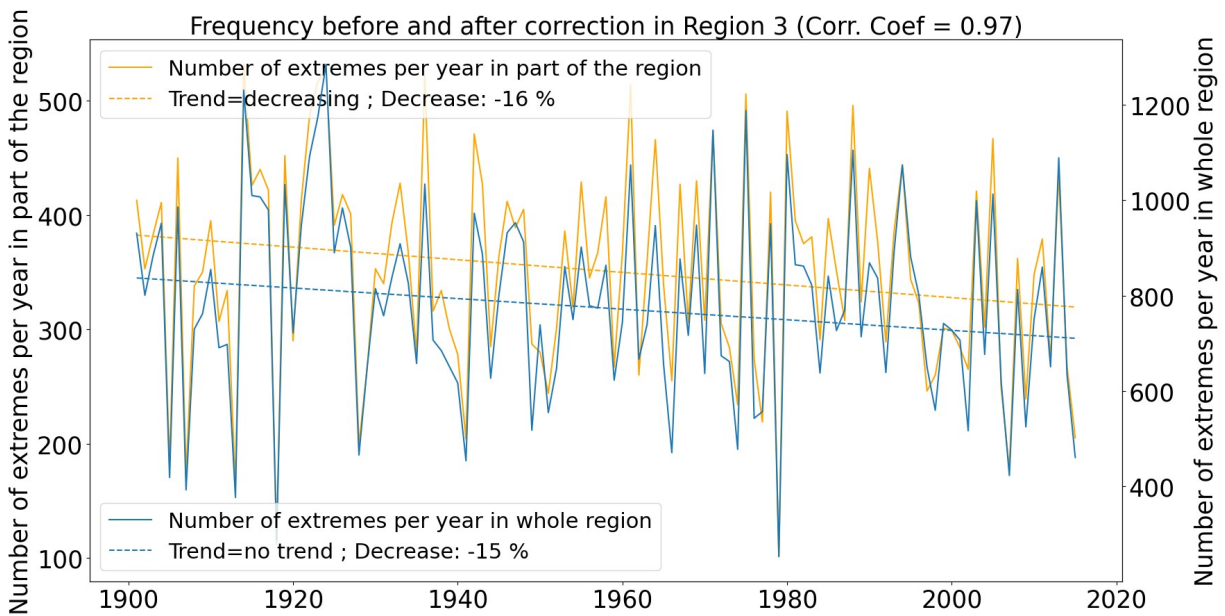
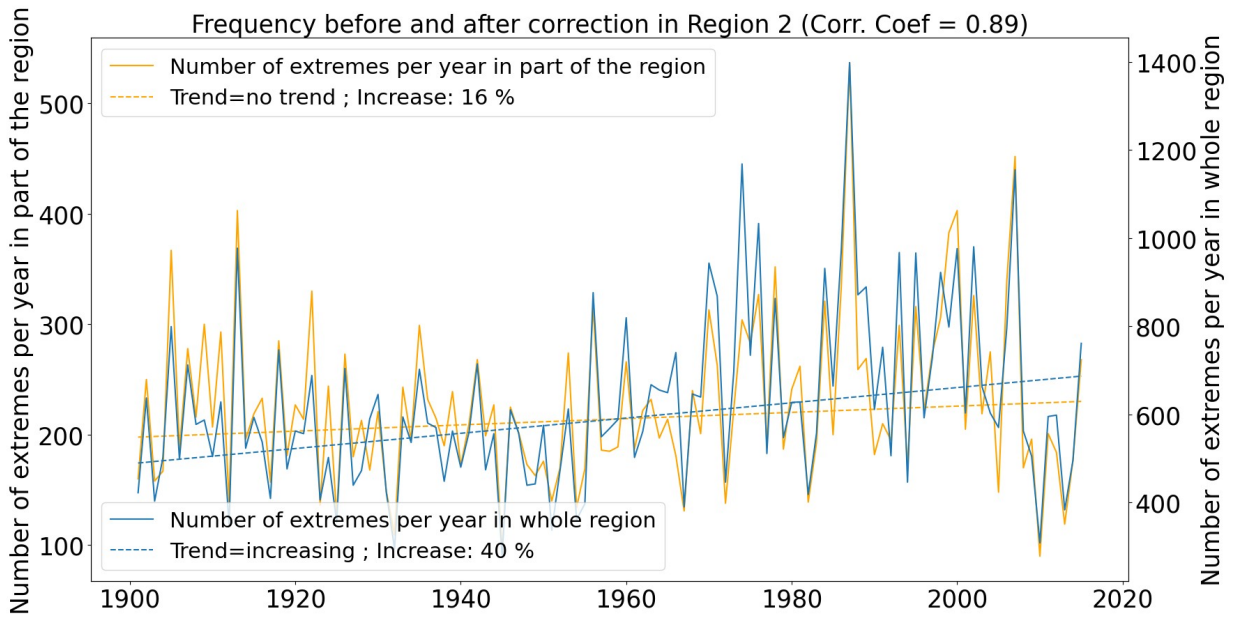
## Supplementary Material

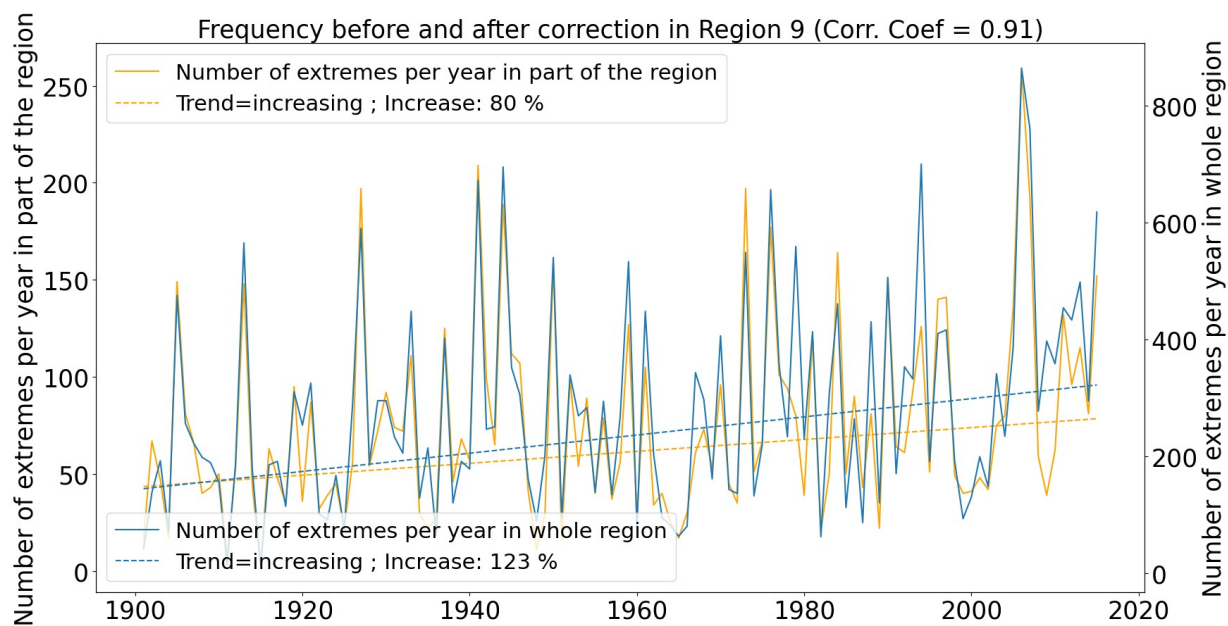
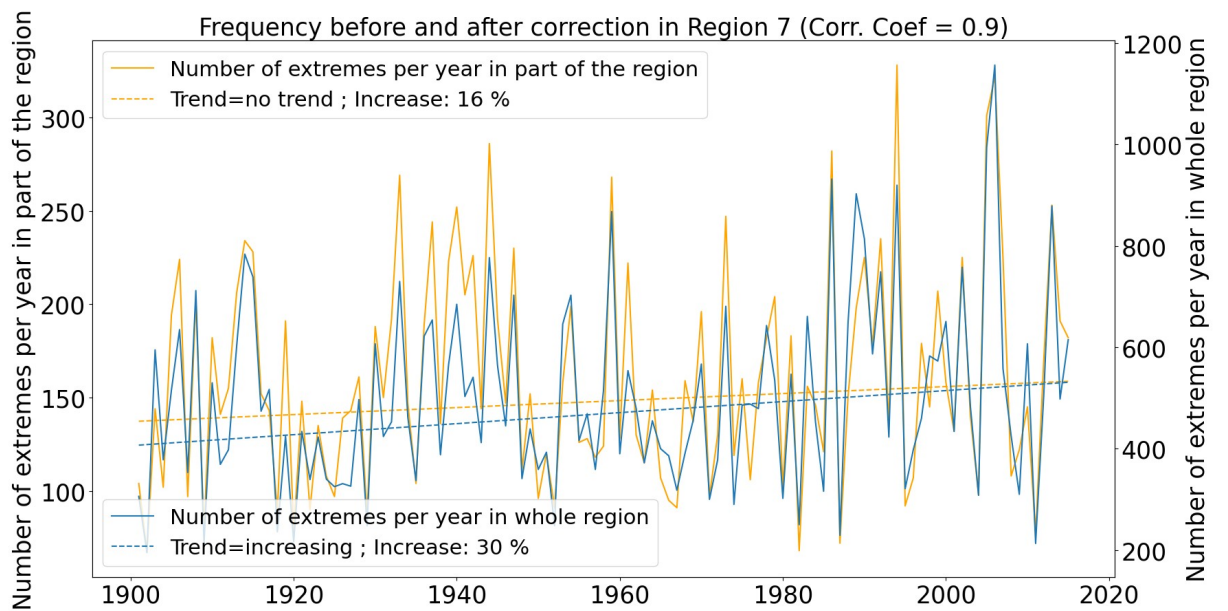
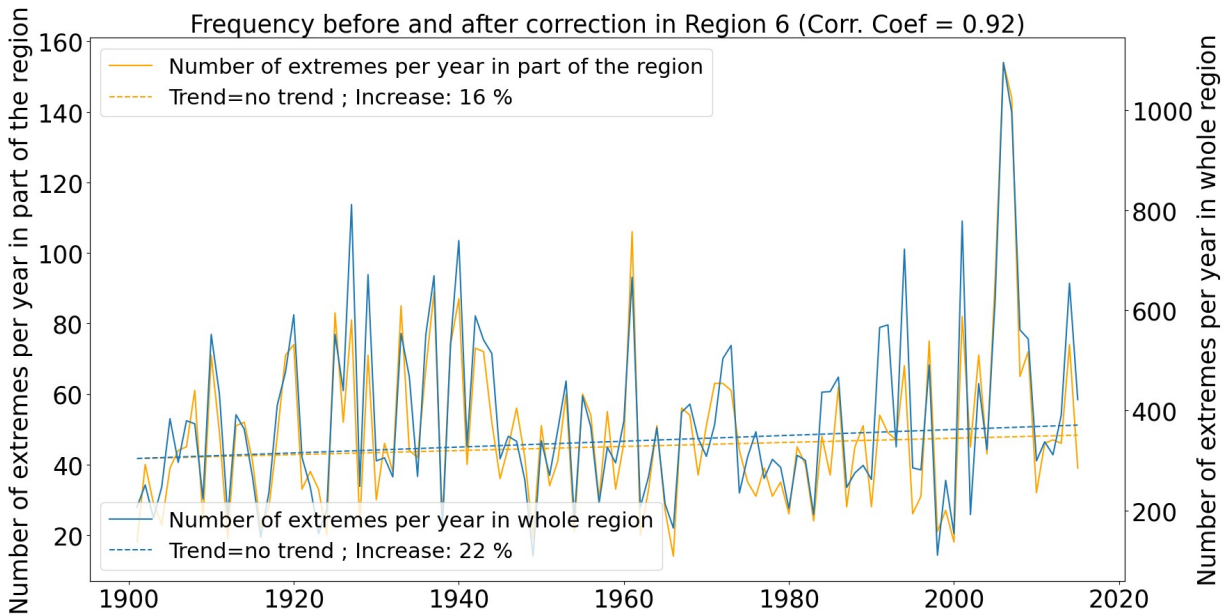


**Fig. S1 | Number of recording stations in regions 4 and 8.** The plots show the total number of recording stations in region 4 (left panel) and region 8 (right panel). We see a sudden increase in the number of recording stations in the 1970's in both regions, which may have had some impact on the resulting calculated extremes. In region 8, there were almost no recording stations in the region until this time. We don't witness such a sudden change in any other region.

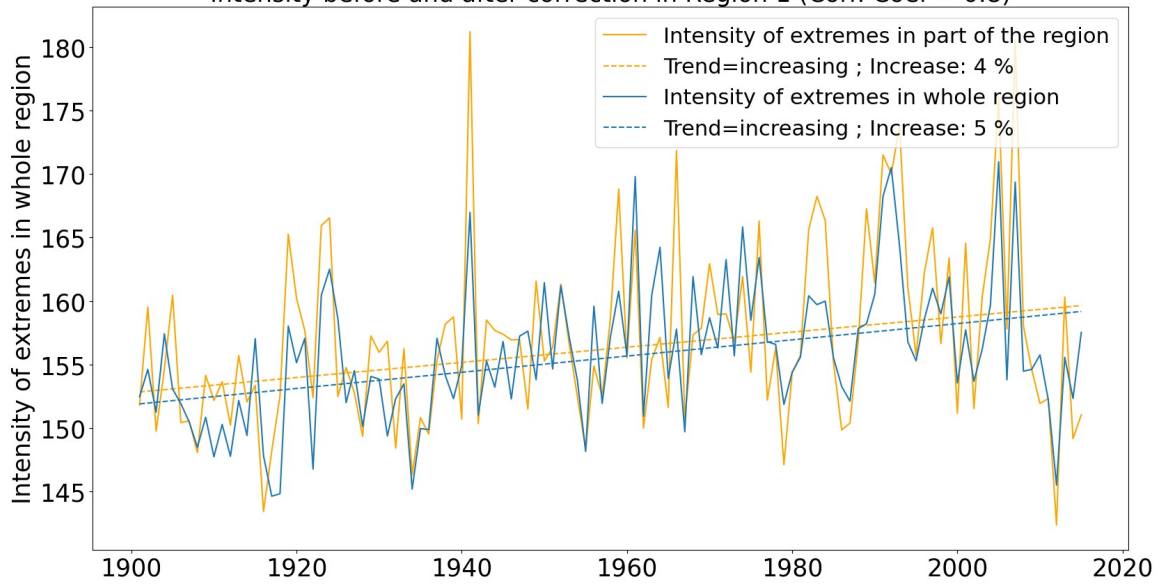




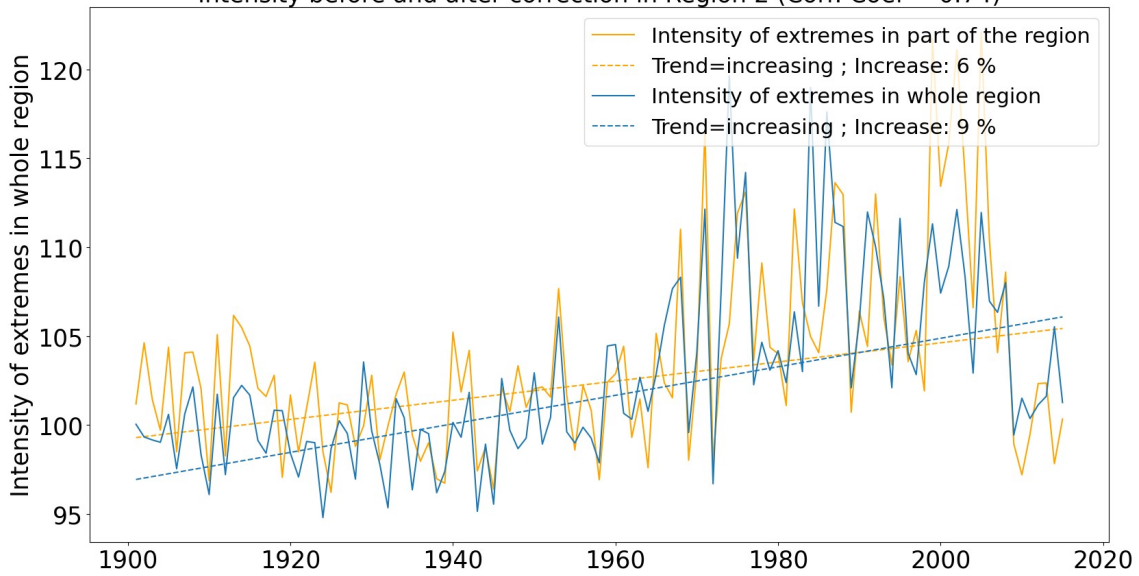




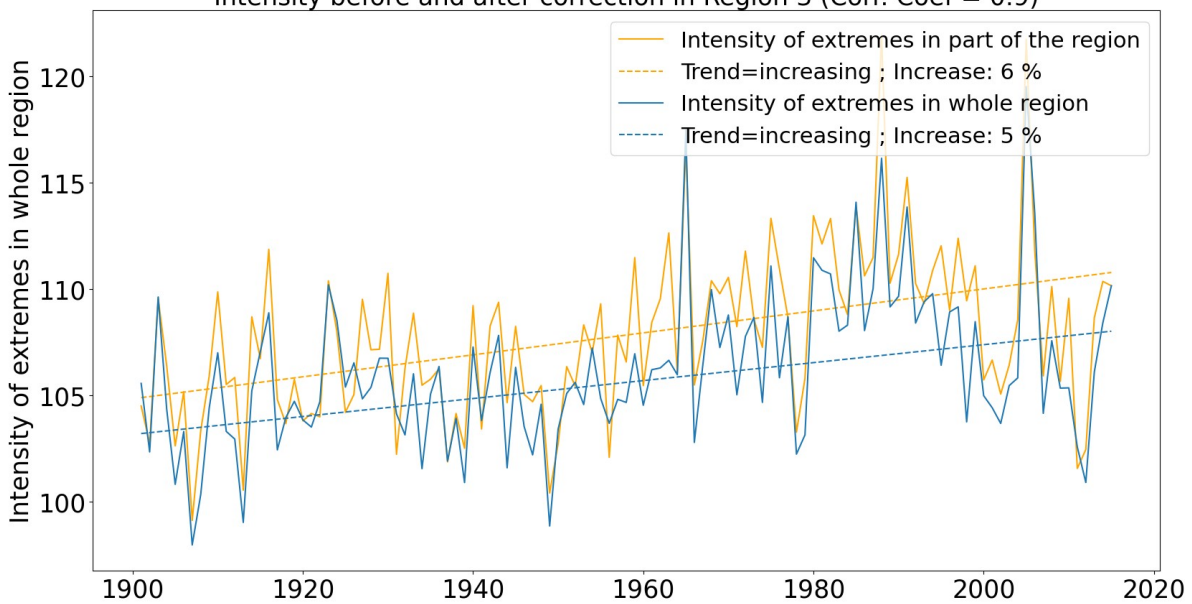
Intensity before and after correction in Region 1 (Corr. Coef = 0.8)



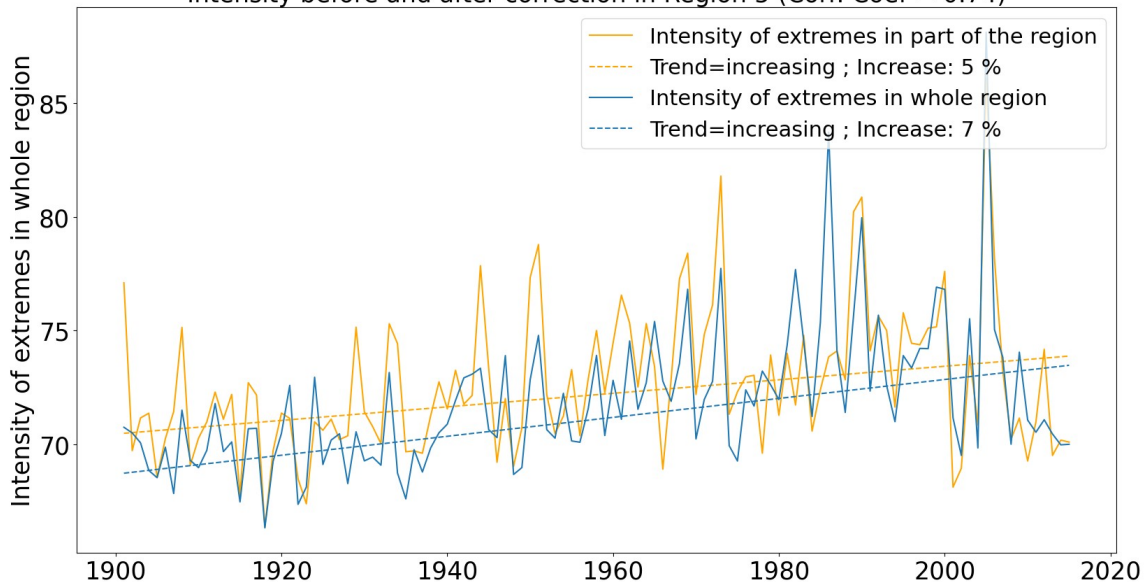
Intensity before and after correction in Region 2 (Corr. Coef = 0.74)



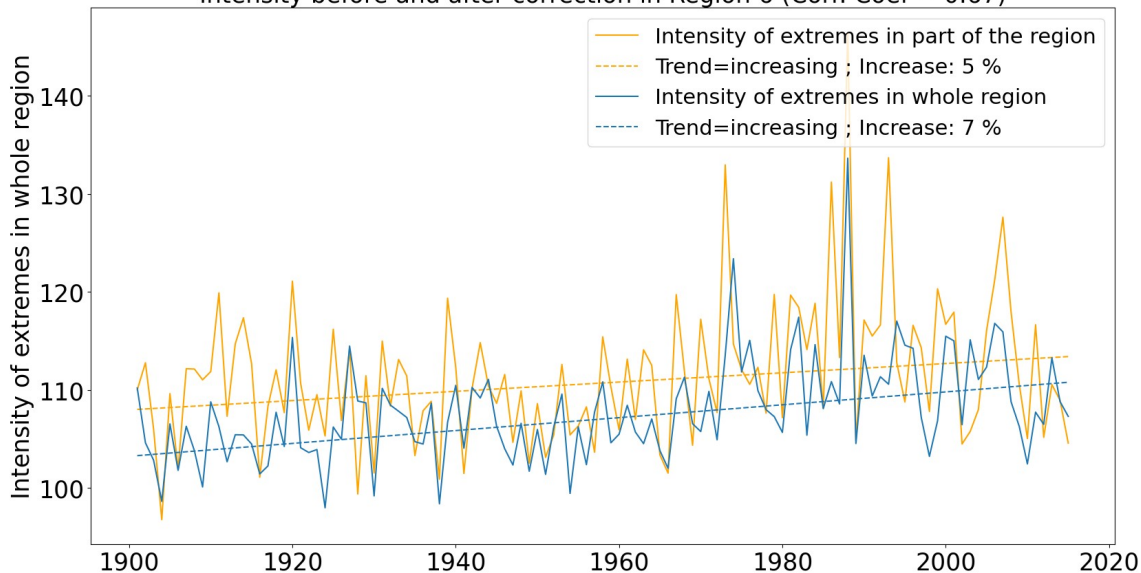
Intensity before and after correction in Region 3 (Corr. Coef = 0.9)



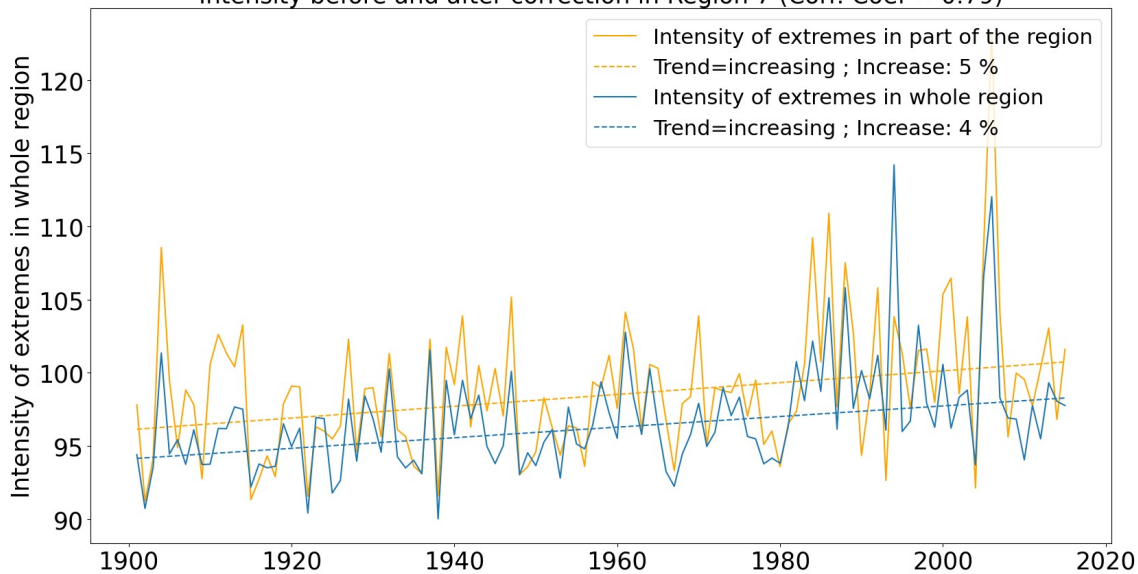
Intensity before and after correction in Region 5 (Corr. Coef = 0.74)

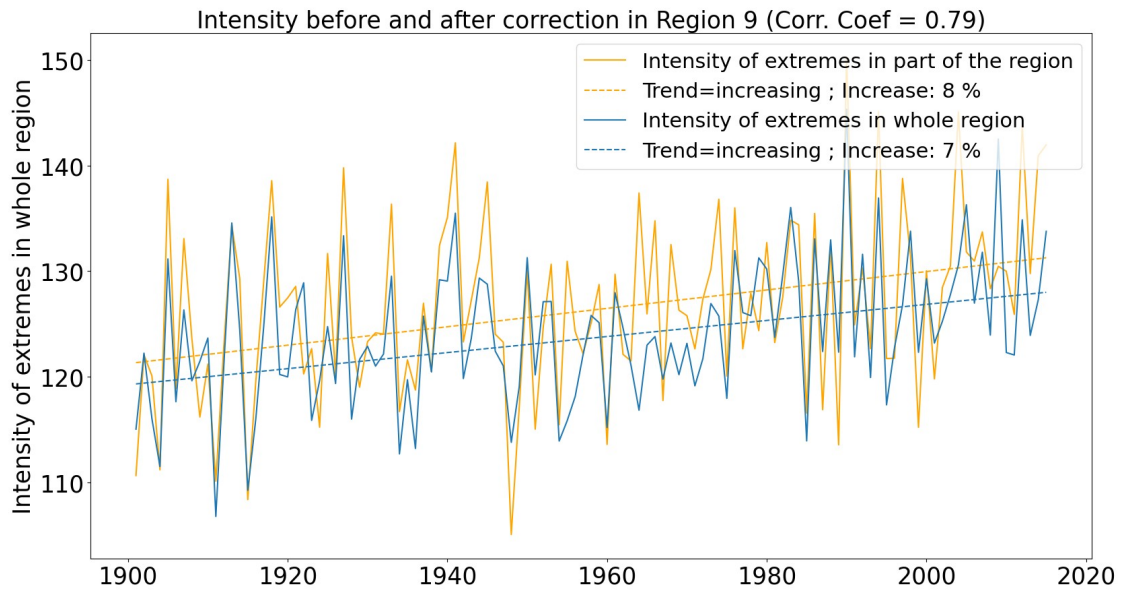


Intensity before and after correction in Region 6 (Corr. Coef = 0.67)

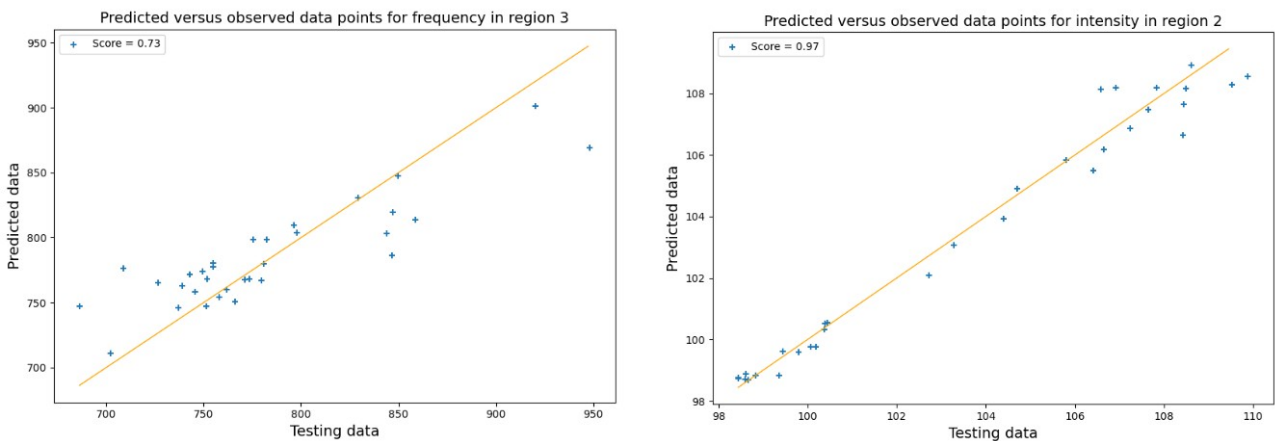


Intensity before and after correction in Region 7 (Corr. Coef = 0.79)

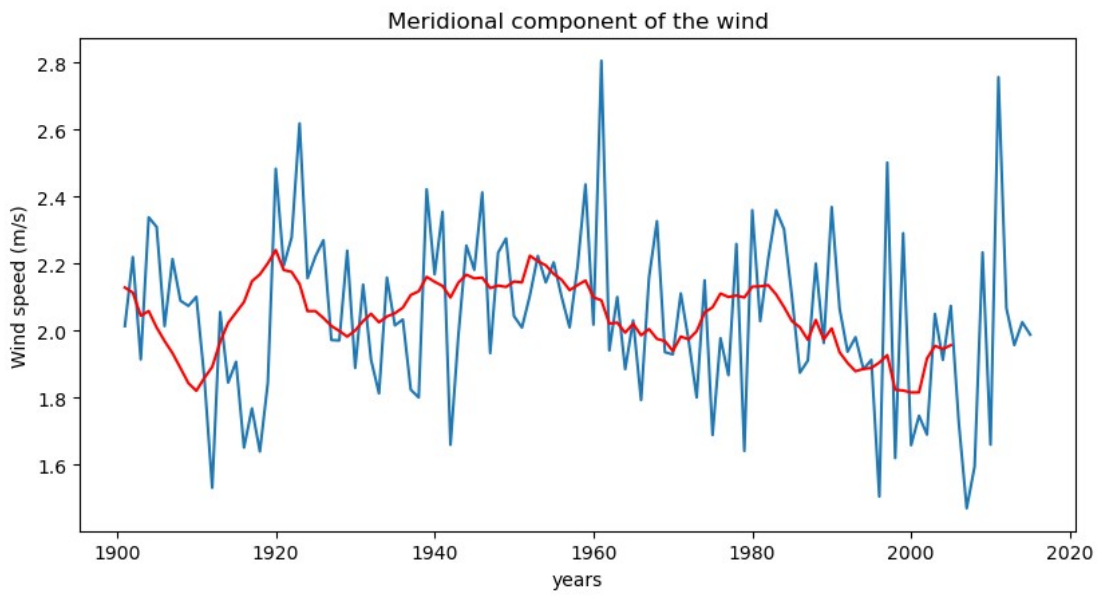
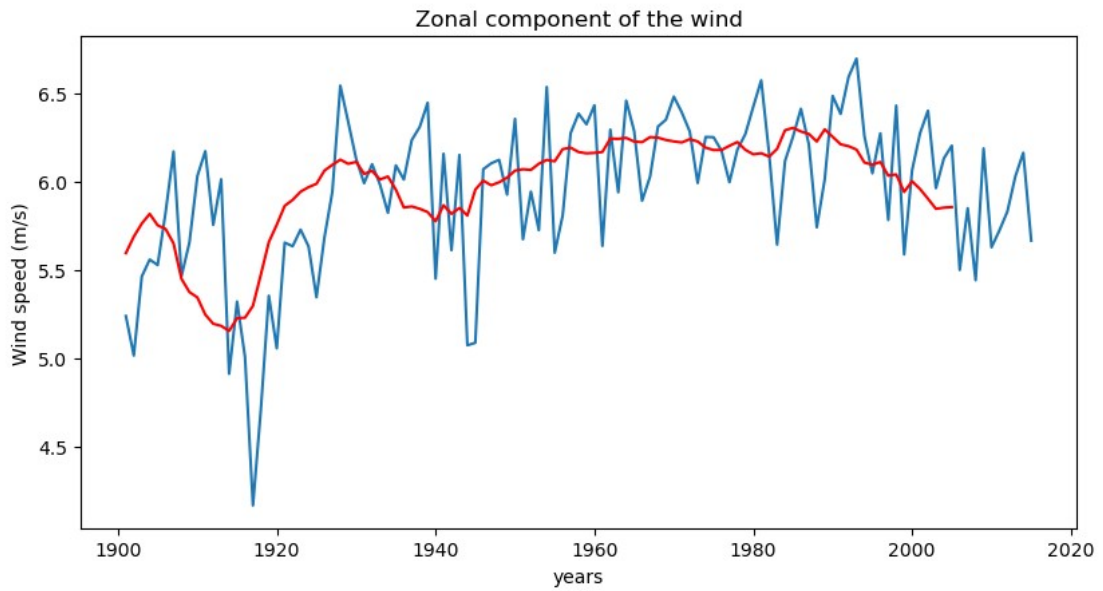
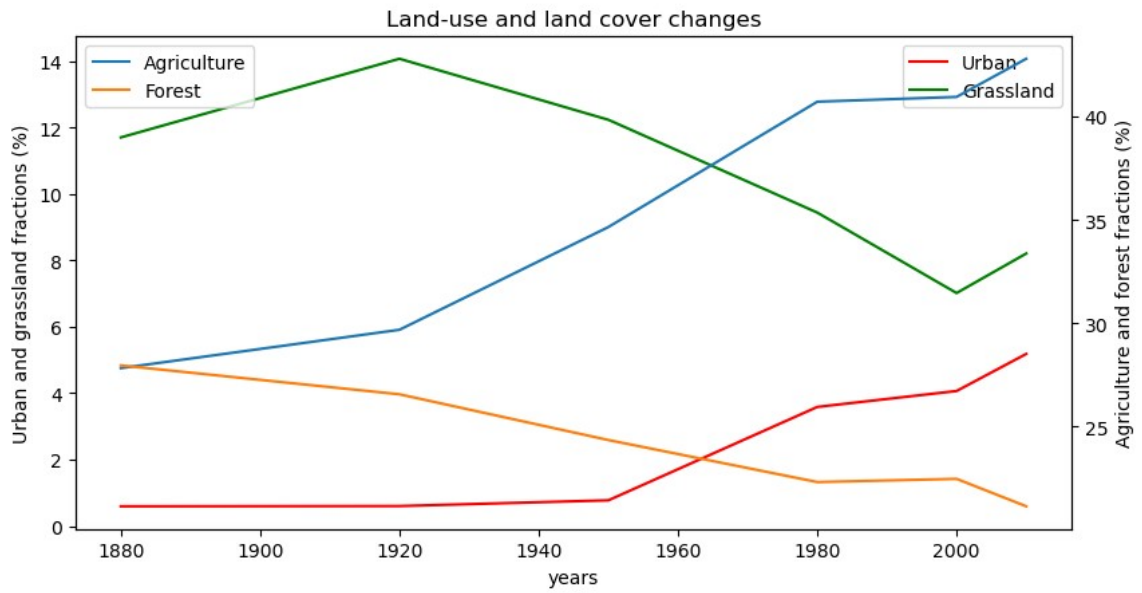




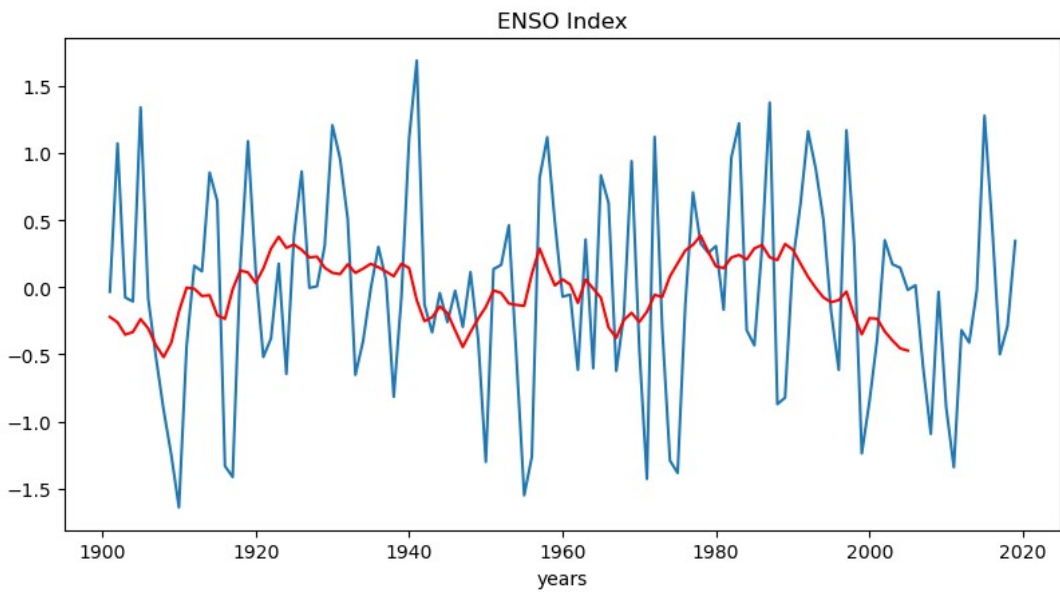
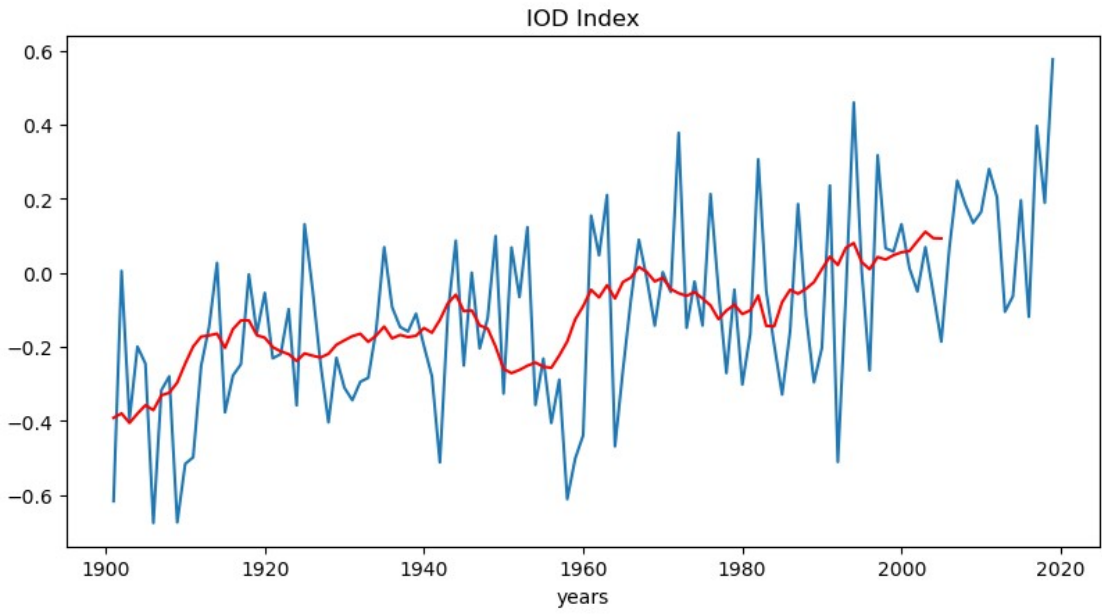
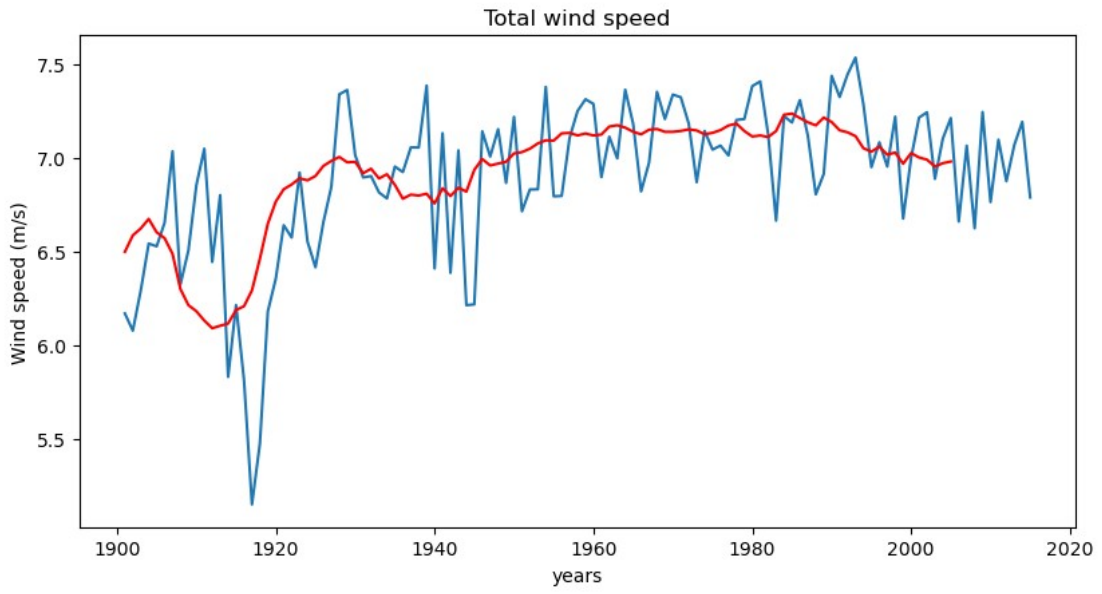
**Fig. S2 | Trend comparison before and after correction on the number of observational stations.** The number of observational stations for the past 120 years has been derived in each region, as well as the number of observational stations when keeping only the grid cells where the number of stations is stable throughout the century (a). The trends of extreme events before and after correction (i.e., using every grid cell in the region versus using only the ones where the number of stations is stable) have been compared (b) in order to assess the impact of the number of recording stations on the trends. The trends before and after correction are found to be similar.



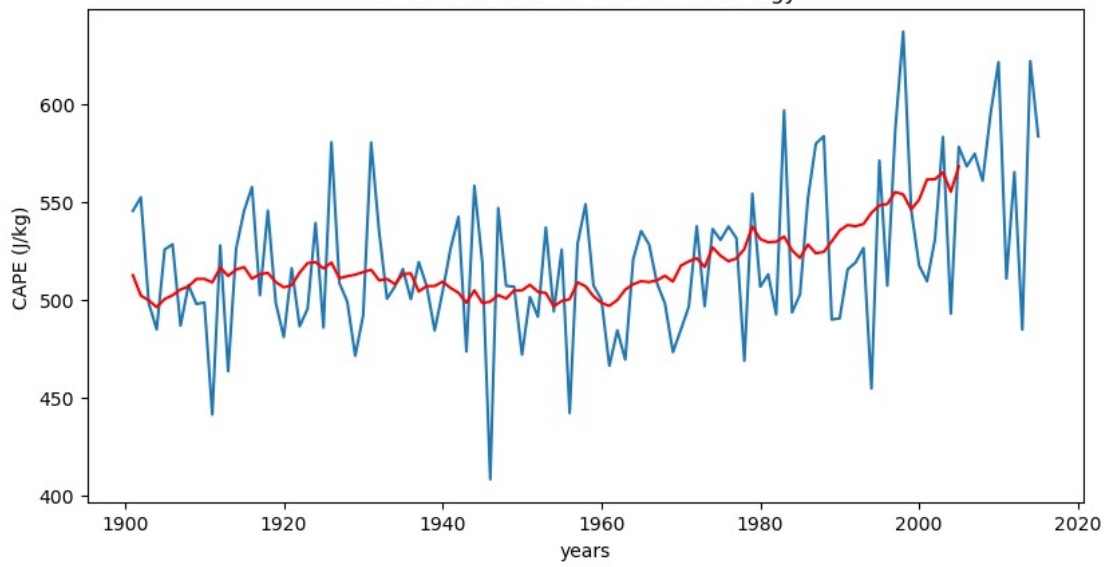
**Fig. S3 | Model prediction versus observation.** Scatter plots of extreme events predicted by the model (y axis) and observations (x axis) for the lowest (left panel) and the highest (right panel) predicting scores. The left panel values of extreme events are given in number of occurrence per year, while the right panel values are given in mm/day. The scatter plots show the results for a single testing subset of the data. The closer the scatter points are to the y=x axis (shown in orange), the more accurate is the prediction.



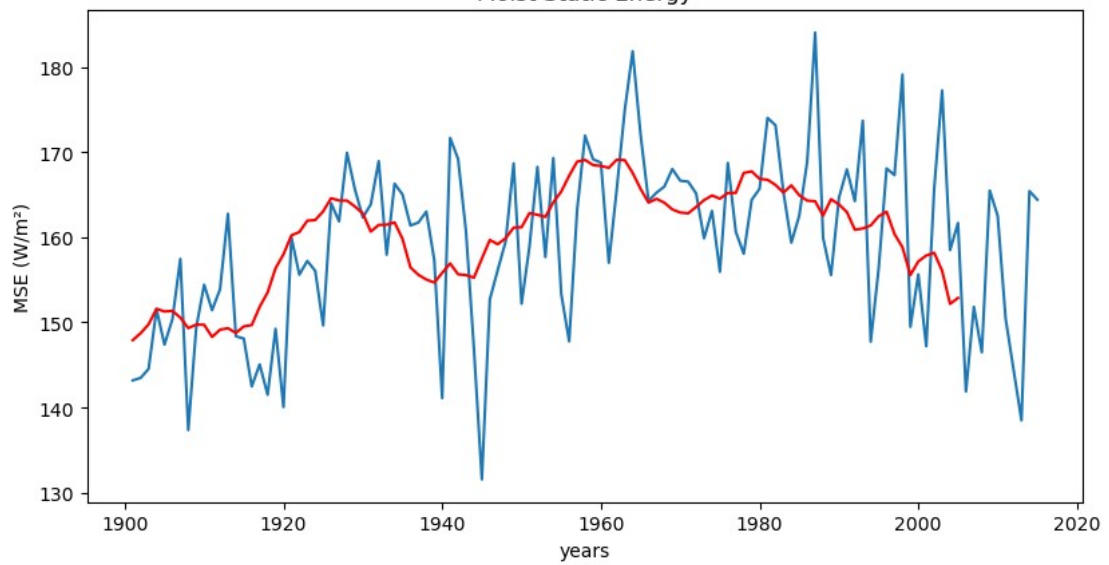




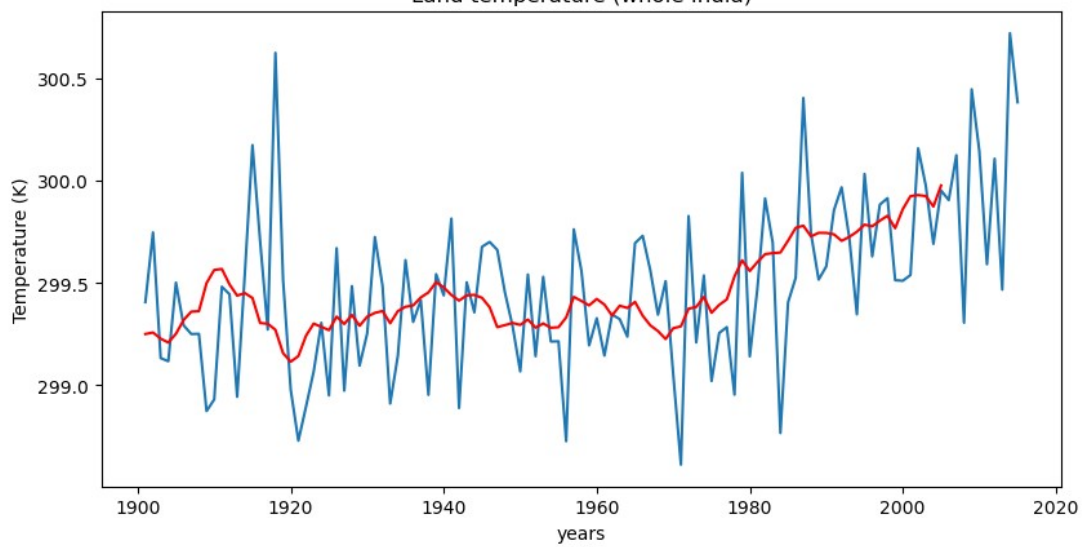
Convective Available Potential Energy

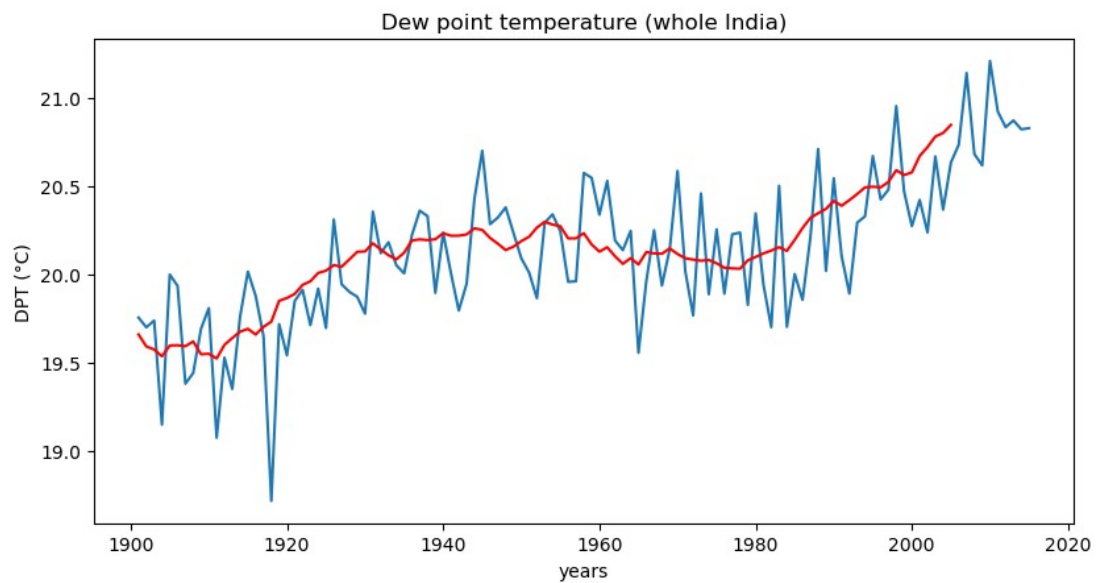
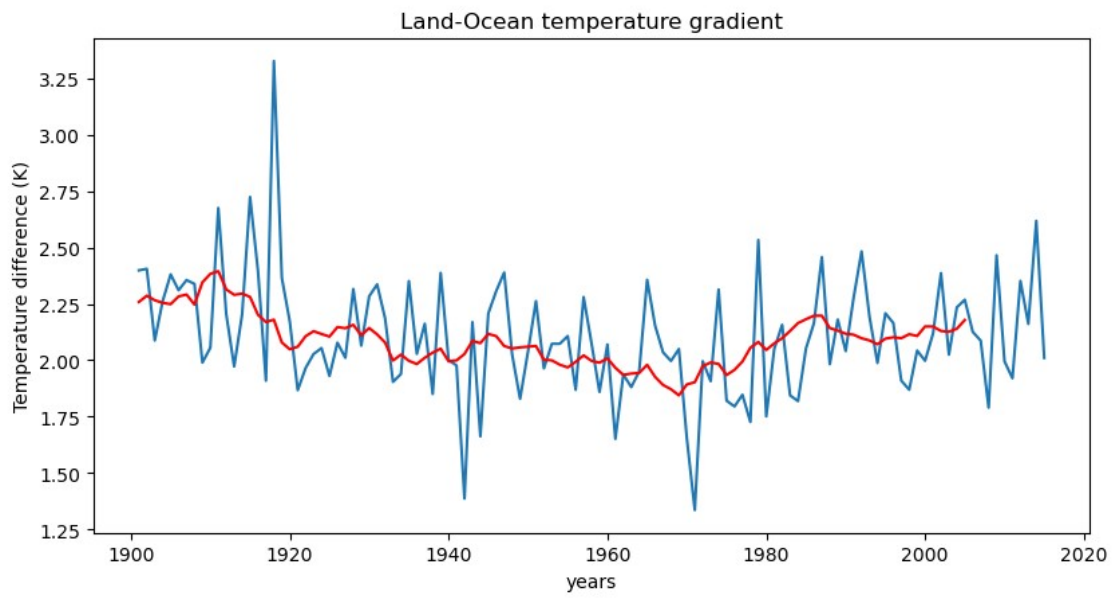
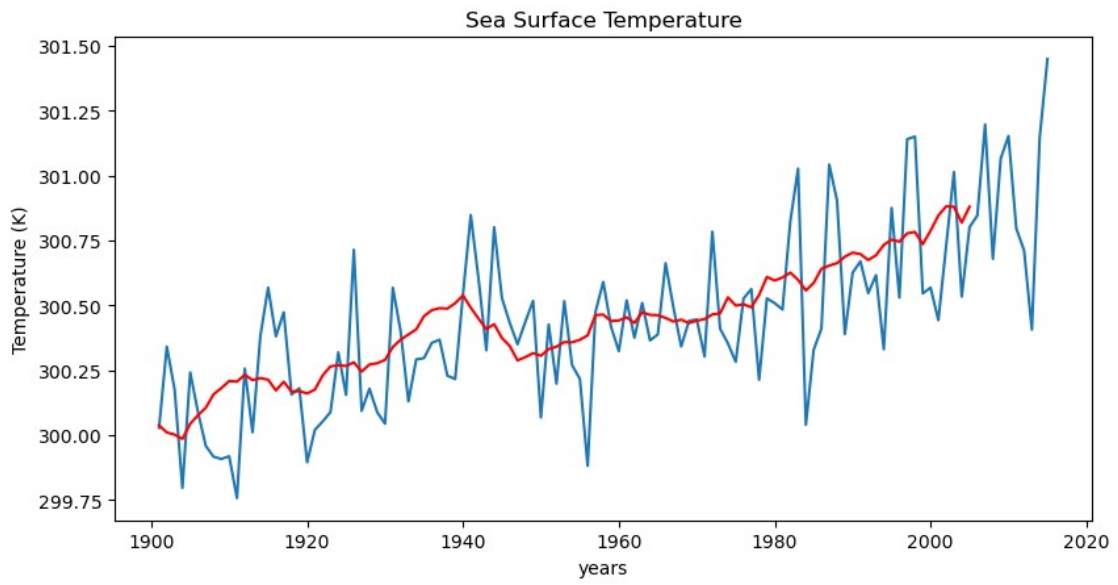


Moist Static Energy



Land temperature (whole India)





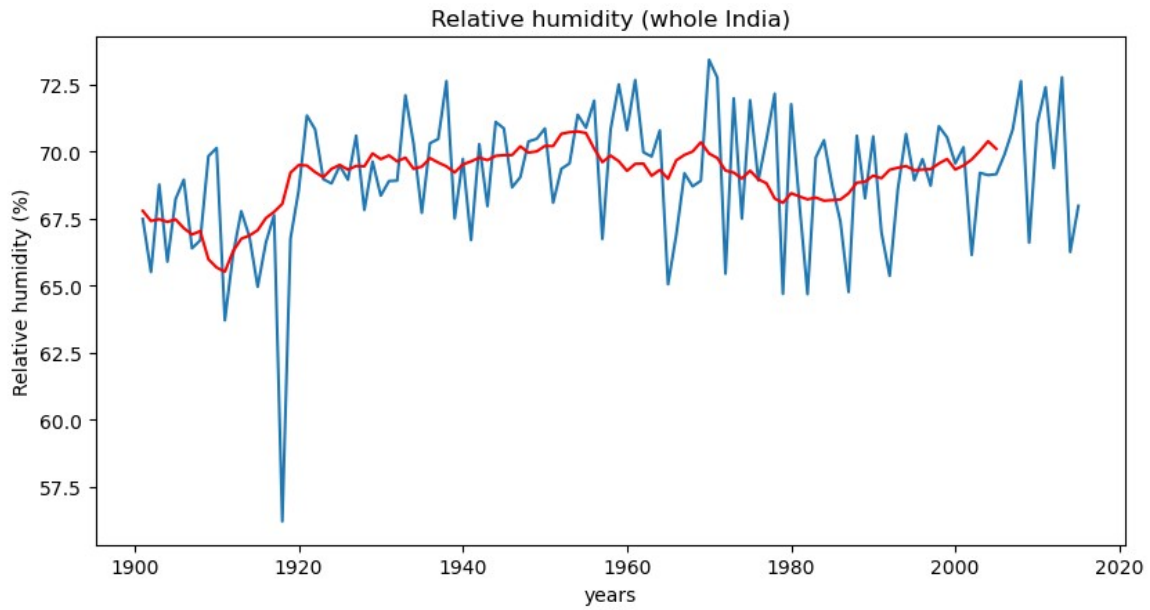


**Fig. S4 | Input features for the Random forest regression.** The time series of the 17 input features used in the random forest regression model are presented. The yearly values are plotted in blue and the 10-year moving averages used in the regression are in red. For the LULC data, we used simple linear interpolation between the different observation data points. For the temperature, dew point temperature, relative humidity and specific humidity, the values averaged over the whole India are shown here, whereas we used regional average in the random forest regression.